Nuclear Instruments and Methods in Physics Research A 693 (2012) 220–225

Contents lists available at SciVerse ScienceDirect

Nuclear Instruments and Methods in Physics Research A

journal homepage: www.elsevier.com/locate/nima

Thin-window gas cell target for activation cross-section measurements relevant for nuclear astrophysics

C. Bordeanu *[,1], Gy. Gyürky, Z. Elekes, J. Farkas, Zs. Fülöp, Z. Halász, G.G. Kiss, E. Somorjai, T. Szücs

Institute of Nuclear Research (ATOMKI), H-4001 Debrecen, POB 51, Hungary

ARTICLE INFO

Article history:
Received 23 May 2012
Received in revised form
18 July 2012
Accepted 18 July 2012
Available online 31 July 2012

Keywords:
Thin window gas cell
Rare noble gas isotope
Nuclear astrophysics
Cross-section measurement
Activation method

ABSTRACT

A thin-window gas target system was designed in order to fulfill the requirements of the measurement of low energy α-induced reaction cross-sections relevant for nuclear astrophysics using the activation method. The properties of the gas cell system, its characterization and the results of the first feasibility studies on the ^{3}He(α,γ)^{7}Be and ^{124}Xe(α,γ)^{128}Ba reactions are summarized.

1. Introduction

In experimental nuclear astrophysics, the cross-section measurements of nuclear reactions, taking place in different stellar environments, play the central role. Ideally, these reactions should be studied at astrophysically relevant energies, which is deep below the Coulomb barrier for charged particles where the cross-sections are extremely small. Since in most of the cases, this is not possible, the cross-sections are usually extrapolated to astrophysical energies from higher energies. However, in order to make the extrapolations more reliable, the measurements must be carried out at energies as low as possible, which requires the determination of low cross-sections in lengthy experiments where the target characteristics are crucial.

In the energy generation and nucleosynthesis processes of stars, reactions involving noble gaseous chemical elements are often encountered. The direct cross-section measurements of these reactions necessitate the usage of gas (or implanted) targets. Two examples, which give the motivation of the present work, are briefly outlined here.

1.1. The ^{3}He(α,γ)^{7}Be reaction

The ^{3}He(α,γ)^{7}Be is one of the key reactions of the so-called pp-chain through which the main sequence stars, like our Sun, generates energy and converts hydrogen into helium. This reaction was studied several times in the past in a wide energy range [1–15]. In one of the most recent experiments, the cross-section of the ^{3}He(α,γ)^{7}Be reaction was measured at relatively high energies $E_{c.m.} = 0.7-3.1$ MeV [15]. A discrepancy was observed between the result of this new measurement and that of an older one carried out in a similar energy range [4]. The obtained cross-sections in Ref. [15] are up to 50% higher than the ones of Ref. [4]. Since in the high energy range only these two datasets are available and theoretical models need to reproduce the cross-section also in this energy range, the discrepancy of the datasets substantially increases the uncertainty of the extrapolated cross-section to stellar energies. Therefore, new measurements of this cross-section in a similar energy range are strongly needed in order to resolve the discrepancy.

1.2. The ^{124}Xe(α,γ)^{128}Ba reaction

The main stellar production mechanism of the heavy proton rich isotopes is the so-called astrophysical γ-process [16]. The modeling of the γ-process requires the knowledge of the reaction rate of thousands of reactions in a wide mass range. Detailed calculations showed that the models were especially sensitive to some specific reactions [17,18], one of them is the ^{124}Xe(α,γ)^{128}Ba reaction. In the astrophysically important energy range (around 10 MeV), no experimental data for this reaction is available and the γ-process models rely on largely untested theoretical reaction rates. Therefore, the cross-section measurement of the ^{124}Xe(α,γ)^{128}Ba reaction is highly important.

* Corresponding author.
E-mail addresses: bordeanu@atomki.hu, bordeanu@tandem.nipne.ro (C. Bordeanu).
[1] On leave from Horia Hulubei Institute of Physics and Nuclear Engineering (IFIN-HH), 407 Atomistilor, Magurele-Bucharest 077125, Romania.

0168-9002/$ - see front matter © 2012 Elsevier B.V. All rights reserved.
http://dx.doi.org/10.1016/j.nima.2012.07.038

1.3. Activation characteristics

Both reactions involve isotopes of noble gases, helium and xenon. The final nuclei are radioactive, thus the cross-section measurements can be carried out using the activation technique. In an activation experiment the cross-section σ is determined in a two step process [19]. First the target with a thickness of T atoms/cm^2 is irradiated for t_i time with a beam having the intensity of ϕ particles per second. The number of the created isotopes at the end of the irradiation is given by the following formula:

$$N = \sigma \cdot T \cdot \phi \cdot \frac{1-e^{-\lambda \cdot t_i}}{\lambda} \quad (1)$$

where λ is a decay constant of the produced radioactive isotope. Then in the second step the activity of the target is determined by measuring a decay radiation. The number of the detected events in a counting period of t_c is given by

$$n = N \cdot e^{-\lambda \cdot t_w} \cdot (1-e^{-\lambda \cdot t_c}) \cdot \varepsilon \cdot \eta \quad (2)$$

where t_w is the time elapsed between the end of the irradiation and the beginning of the counting, η is the intensity per decay of the measured radiation and ε is the detection efficiency for that radiation.

^{7}Be decays by electron capture with a half-life of 53.22 d [20] and the decay is followed by the emission of a 478 keV γ-radiation. Similarly, ^{128}Ba has a half-life of 2.43 d [21] and its decay involves the emission of a 273 keV γ-ray. If the reaction products can be collected in a suitably designed gas target, the subsequent measurement of the γ-activity can be used to determine the reaction cross-section.

The aim of the present work was to design and develop a thin-window gas cell, which can be used to study both reactions with only minor modifications. With the gas cell the ^{3}He(α,γ)^{7}Be cross-section is to be measured between about 4 and 7 MeV α-energies where the strong discrepancy of the available experimental data is present. The study of the ^{124}Xe(α,γ)^{128}Ba reaction is planned in the 10–15 MeV energy range, relevant to astrophysics γ-process temperatures.

2. The gas cell design

There are essentially three different ways to produce targets for cross-section measurements from isotopes of noble gaseous elements: implanting the gas into a solid material, gas target confined into a window closed volume and windowless gas target.

The target atoms can be implanted into a suitable target backing. In this case the experiments are carried out using a solid state target. Though achievable isotopic purity is 100%, implanted targets have several disadvantages. The achievable target thickness (the number of target atoms per unit area) is limited by the maximum number of implanted atoms the backing can hold (e.g., due to the blistering effect [22]). The determination of the target thickness is rather difficult and care must be taken to preserve the target stability under beam bombardment [3]. This problem is especially severe for noble gas atoms which can diffuse out easily from the backing [23].

The gas targets can be grouped into two categories: windowless gas targets and gas cell targets. The windowless gas targets (either extended [6,9] or jet type [24,25]) are useful when the entrance window must be avoided. This is the case when the experiments are carried out at such low energies that even the thinnest possible window would degrade and scatter the beam energy too much. The windowless target is also needed when the disturbing radiation induced in the window would bury the weak signal from the studied reaction (as in in-beam γ-spectroscopy measurements of low cross-sections). In addition, the windowless gas target systems need much more complicated experimental setups involving, e.g., several pumping stages.

If the conditions of the measurement do not require windowless gas target, the gas cell is an option. If the studied energy range is high enough, a thin entrance window of the target cell can be used; this is the case of this study too. In case of the activation method, the beam-induced background of the entrance foil does not play a role. The other advantage of the gas cell is that, with a carefully designed cell, only a little amount of gas is necessary.

In our case, both studied reactions involve very rare isotope targets (the natural abundance of ^{124}Xe is about 0.1%, while that of ^{3}He is as low as 1.3×10^{-4}%), therefore, the target gases are very expensive. A windowless gas target – even if gas recirculation is implemented – typically consumes more gas than needed for a small gas cell, which results in an increased cost of the experiments.

Taking into account the above facts, a thin-window gas cell for the study of the ^{3}He(α,γ)^{7}Be and ^{124}Xe(α,γ)^{128}Ba reactions was designed. Fig. 1 shows the schematic layout of the gas cell and the target chamber to which the cell was connected.

The target chamber can be attached to the beamline either of the cyclotron or of the Van de Graaff accelerators of ATOMKI. The chamber together with the gas cell was insulated from the rest of the beamline and from other elements of the setup, thus the number of projectiles entering the chamber could be determined by measuring the electric beam current. The beam entered the chamber through a variable diameter aperture, on which the beam current could also be measured (and thus minimized). Behind the entrance aperture, a larger diameter aperture was put which was not hit by the beam. In order to make the measurement of the beam current reliable, a -300 V voltage was applied to this aperture to suppress the escape of the secondary electrons from the chamber. Increasing the voltage above 300 V did not affect the current reading any more, thus with this voltage the secondary electrons were totally suppressed.

An ion implanted Si detector was placed into the chamber to detect the backscattered α-particles from the gas cell entrance foil and the target gas. This was used to monitor the beam position, the stability and purity of the entrance foil and that of the target gas (see the details in Section 4).

The gas target itself is a cylindrical cell. Both the length and the radius were 10 mm for the Xe cell, while for the ^{3}He case both length and diameter were 30 mm. The beam entered the cell

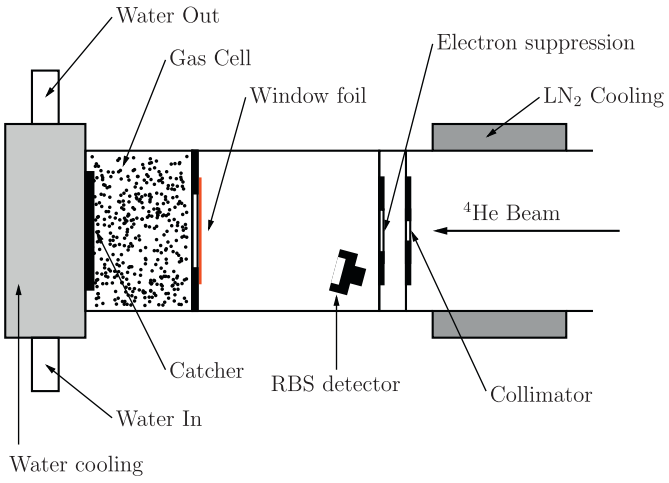

Fig. 1. Schematic layout of the target chamber and gas cell. The system components are discussed in the text.

through a thin entrance foil which could be of various thickness and diameter. The beam impinged on a directly water cooled beam stop at the back of the cell on which the catcher for the produced radioactive isotopes was attached. Various materials could be used as catcher, see Section 3.2.

Several ports were placed along the mantle of the cylinder implemented with thin 4.15 mm inner diameter tubes in order to keep the whole volume of the gas cell minimal, using standard Swagelok parts. One port is connected to a (25 cm^3) gas bottle from which target gas could be let into the cell through a needle valve. One port was connected to an MKS Baratron (type 722B) to measure the pressure of the target gas. A third port was connected to a vacuum system which could be used to evacuate both the chamber and gas cell before filling the cell with target gas.

The cell was made in a modular design. All parts including the entrance foil and catcher could be easily replaced and therefore the system could be adjusted to the different needs of the $^{3}He(\alpha,\gamma)^{7}Be$ and $^{124}Xe(\alpha,\gamma)^{128}Ba$ experiments.

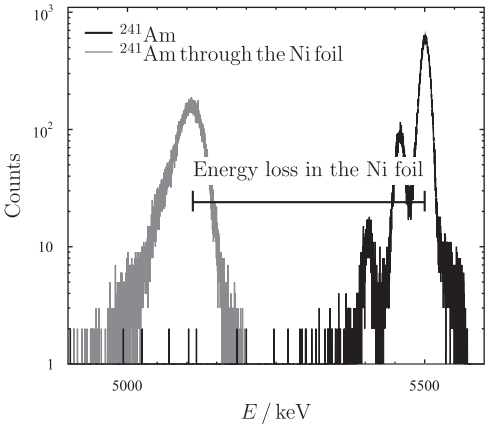

Fig. 2. Typical α-spectra used to determine the Ni entrance foil thickness and uniformity. Due to the energy straggling in the foil, the peak is much broader and the three peaks are not resolved.

3. Characterization of the gas cell components

3.1. Entrance window properties

One of the most important components of a gas cell system is the thin entrance foil. The foil to be used should meet several requirements. It must have high mechanical and thermal stability. The mechanical stability is needed so the foil holds the pressure inside the gas cell (the maximum pressure in our case was about 400 mbar). Since it is continuously bombarded by the beam, the foil must be resistant to the induced heat. It must be free of pinholes as well so that the target gas is not lost from the chamber.

One of the crucial points of the entrance window is its thickness. It must be thin enough to cause little energy loss of the beam. This requirement depends on the reaction to be studied: the combination of the beam energy, projectile and foil material atomic number and mass. From the two reactions to be studied, the $^{3}He(\alpha,\gamma)^{7}Be$ puts a stronger constraint on the foil thickness. Since the aimed α energy range is 3–7 MeV, the energy loss, the energy and angular straggling must be kept minimum in this energy range. One commonly used material for gas target entrance foil is nickel. We used pinhole-free 1 μm thick foils provided by LeBow company [26] for the $^{3}He(\alpha,\gamma)^{7}Be$ measurements. The foils were fixed onto 8 mm diameter stainless steel frames.

The $^{124}Xe(\alpha,\gamma)^{128}Ba$ reaction is to be studied in the α energy range 10–15 MeV. In this energy range the stopping power is lower and consequently thicker windows can also be used. Pinhole free, 6 μm thick Al foil produced by Goodfellow [27] was chosen as the entrance window for the ^{124}Xe experiment.

For the precise knowledge of the interaction energy, the beam energy loss in the entrance window and therefore the exact thickness of the foil must be known. Thus, the nominal thickness quoted by the manufacturer was checked. The measurement of the thickness uniformity was also important to assess the energy straggling of the beam after passing through the foil.

The foil thickness and uniformity was determined through the measurement of the energy loss of α-particles in the foil using an ORTEC SOLOIST α-spectrometer [28]. The Si detector energy calibration was done with a triple α-source containing ^{239}Pu (with α-energies of 5105.5 keV, 5144.3 keV and 5156.59 keV), ^{241}Am (5388.23 keV, 5442.8 keV, 5485.56 keV) and ^{244}Cm (5762.7 keV, 5804.82 keV). Then, a single, collimated ^{241}Am source was put in the spectrometer and its spectrum with well separated three peaks was measured with the Si detector. The entrance window was then placed between the source and the detector. Owing to the energy straggling of the α-particles in the foil, the three peaks cannot be resolved. The broad peak was fitted with the sum of three Gaussians with the appropriate energy separations and intensity ratios. From the obtained difference of the measured α-energies, the thickness of the foil could be obtained. Fig. 2 shows an example of the measured α-spectra.

By measuring the thickness at several positions of the foil, the uniformity of the window could be checked. The average energy loss of the 5485 keV α-particles from the ^{241}Am source was 397 keV. According to SRIM simulations [29] this corresponded to a foil thickness of 1.01 μm, in perfect agreement with the 1 μm quoted by the producer. Measurements at nine different positions on an 8 mm diameter Ni window, using a 2 mm diameter collimator for the α-source, resulted in the same thicknesses within 2%. A total uncertainty of 4.1% has been assigned to the foil thickness determination which is the quadratic sum of the 2% inhomogeneity, 1% of the determination of the energy shift, and 3.4% of the stopping power values from the SRIM code.

A similar procedure was followed with the 6 μm Al foil used for the Xe experiment. Here the average thickness was found to be 6.57 μm with a standard deviation of 0.06 μm based on the measurement at five different positions. It has to be noted, however, that in the case of the Xe experiment the precise thickness and homogeneity of the entrance window is less important compared to the ^{3}He measurement. For a 10 MeV α-beam the obtained 0.06 μm inhomogeneity of the foil translates to an energy uncertainty of less than 10 keV which is negligible regarding the weak energy dependence of the $^{124}Xe(\alpha,\gamma)^{128}Ba$ cross-section.

3.2. Selection of the catcher

When the reaction products are created along the gas cell in the fusion process, wherever they formed, they have enough energy to reach the end of the cell and get implanted into that part of the cell called the catcher. The catcher is part of the gas cell which is replaced for each experiment. At the end of the irradiations, it was removed and the γ activity was measured off-line.

Since the cross-sections are to be measured with the activation method, the selection of the catcher material which is used to collect the produced radioactive nuclei is of high importance. Since the catcher is directly bombarded by the beam, its material must be suitably chosen in order not to produce any long-lived radioactive isotope inside, which may disturb the off-line γ-measurement of the studied reaction products. Since the reaction products reach the catcher with relatively low energy, the

elastic backscattering can be non-negligible. In order to avoid losses of activity by backscattering, low atomic number catcher is preferred.

To study the beam-induced activity, thick high-purity (99.99%) Oxygen-Free High Conductivity (OFHC) copper sheets from Advent Research Material [30] were irradiated with intense α-beams from the accelerators of ATOMKI, at the Van de Graaff at 3.8 MeV and at the cyclotron at 8.0 MeV. After the irradiations, the activity of the targets were measured with a 100% relative efficiency HPGe detector equipped with complete 4π low-background shielding. No disturbing activity was observed above the laboratory background level, therefore, the OFHC copper was chosen for the catcher material in the ^{3}He(α,γ)^{7}Be experiment.

Copper is also a good choice from the backscattering loss point of view. In order to study this effect, SRIM [29] simulations were carried out using the conditions of the ^{3}He(α,γ)^{7}Be experiment with different catcher materials. The results of such a simulation can be seen in Fig. 3 where Pt was also included for comparison. The backscattering loss was much less for Cu, and in the energy range of the planned ^{3}He(α,γ)^{7}Be experiment (^{7}Be energies over 1.0 MeV) the backscattering loss was below 0.1%, therefore, could be neglected.

For the ^{124}Xe(α,γ)^{128}Ba experiment, copper is not recommendable as catcher material because the higher α-energies needed for this reaction cause high activities of ^{66}Ga, ^{67}Ga and ^{68}Ga which can disturb the detection of the ^{128}Ba decay. Therefore, 20 μm thick Al foil attached to the water cooled Al cell bottom was used to collect the created ^{128}Ba isotopes. As opposed to the ^{3}He(α,γ)^{7}Be case, thin catcher foils were preferred here because due to the large mass difference the reaction products were fully stopped in the catchers but the α-beam lost only a small part of its energy, hence, the production of disturbing activity on impurities was less likely. The test measurements proved that the Al foil has only short half-life products so the amount of disturbing activity induced was tolerable. According to the reaction kinematics, only forward scattering of ^{128}Ba isotopes can occur on Al nuclei, therefore, the backscattering loss was not relevant for the ^{124}Xe(α,γ)^{128}Ba reaction.

4. Test measurements with α-beam

4.1. Irradiations

The gas target cell in the configuration for both the ^{3}He(α,γ)^{7}Be and ^{124}Xe(α,γ)^{128}Ba experiments was tested at the cyclotron accelerator of ATOMKI. The cell was filled with either about 300 mbar ^{3}He (99.95% enrichment) or about 50 mbar ^{124}Xe gas (99.97% enrichment). During the irradiations no further gas was added to the cell, but the pressure was monitored continuously. The temperature of the gas was also monitored by fixing a contact thermometer to the mantle of the cell.

Test irradiations of up to 24 h duration were carried out with typical He^{++} beam intensities of 0.4 eμA (^{3}He(α,γ)^{7}Be case) and 1 eμA (^{124}Xe(α,γ)^{128}Ba case). As an example, Fig. 4 shows the pressure variation in the ^{3}He gas cell during and after the irradiation. The pressure variation during the irradiation was less than 3%.

As mentioned in Section 2, a particle detector was placed into the chamber for the detection of backscattered projectiles and for the monitoring of the target gas and/or entrance foil. The scattering on the heavy ^{124}Xe target gas could directly be observed in the backscattering spectrum. The continuous measurement of the scattering spectrum along with the charge integrations made it possible to monitor the quantity of the Xe target gas in the cell. Besides the pressure measurement, this provided an independent control of the amount of the target gas.

In the case of the ^{3}He(α,γ)^{7}Be measurement, on the other hand, owing to the mass relation of the target and projectile, only the α-particles scattered from the Ni window could be detected, therefore, only the stability of the window could be monitored.

Fig. 5 shows typical backscattering spectra for the two measurements. The upper panel represents the ^{3}He case. Along with the Ni foil plateau, a peak corresponding to the carbon contamination of the foil is indicated. By the measurement of the growth of the carbon peak, the carbon built up on the foil from the vacuum system could be monitored. In the lower panel, a spectrum for the Xe gas cell can be seen. The elastic scattering

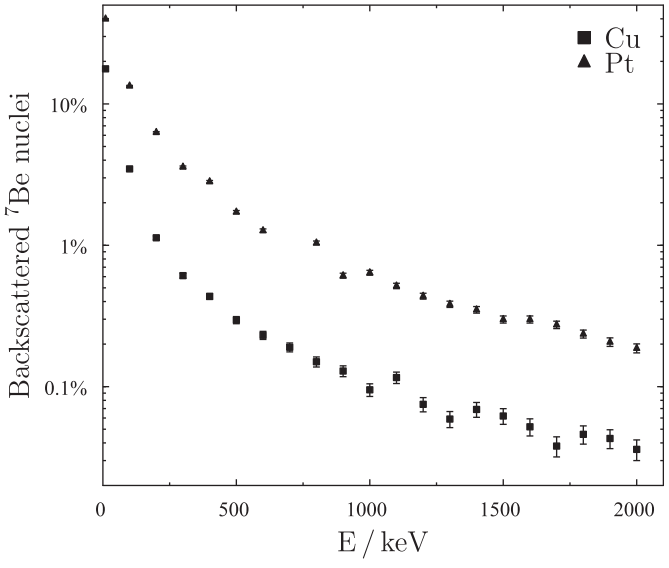

Fig. 3. Simulated ^{7}Be backscattering loss on Pt and Cu catcher material using the SRIM code [29]. The backscattering loss from Cu is below 0.1% in the whole ^{7}Be energy range above 1.0 MeV. The error bars represent the statistical uncertainty based on the square root of the number of backscattered events obtained in the SRIM simulation.

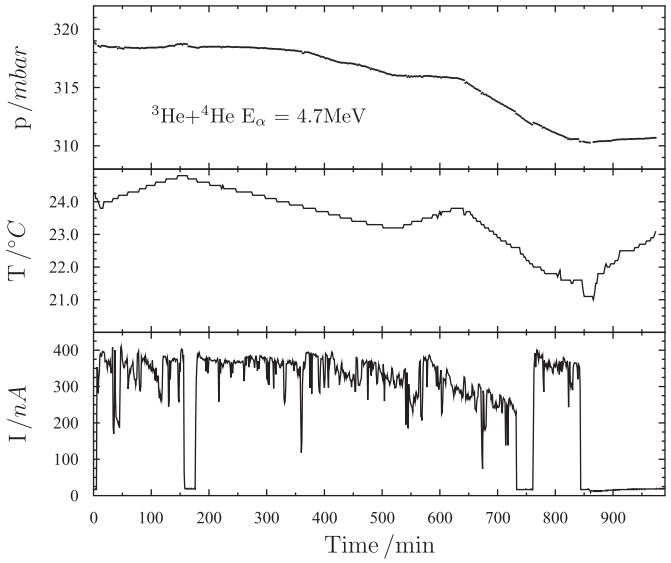

Fig. 4. Pressure variation in the ^{3}He gas cell during and after the irradiation (upper panel). Note the suppressed pressure scale. The overall pressure variation is not more than 3%. The gas pressure varies mainly according to the cooling water temperature, which is not constant, and is very little affected by the current variations. Temperature was monitored on the top of the gas cell body and its time variation is shown in the middle panel. For a more complete picture the variation of the beam intensity in the same time period is also shown in the lower panel.

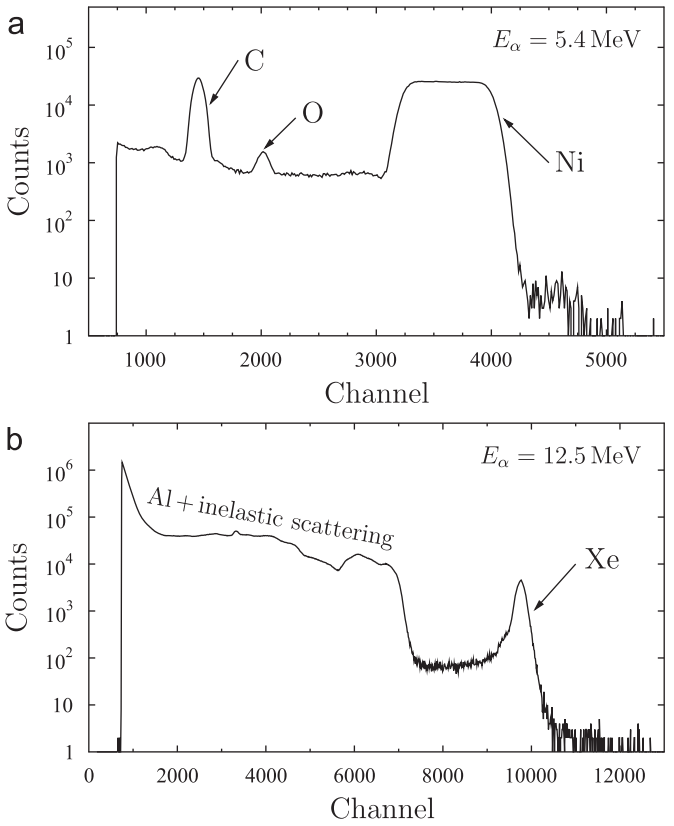

Fig. 5. Backscattering spectra. Upper panel: He gas cell, where only the Ni window (and its carbon deposition) is detectable. The oxygen comes from H_2O molecules present into the vacuum. Lower panel: Xe gas cell.

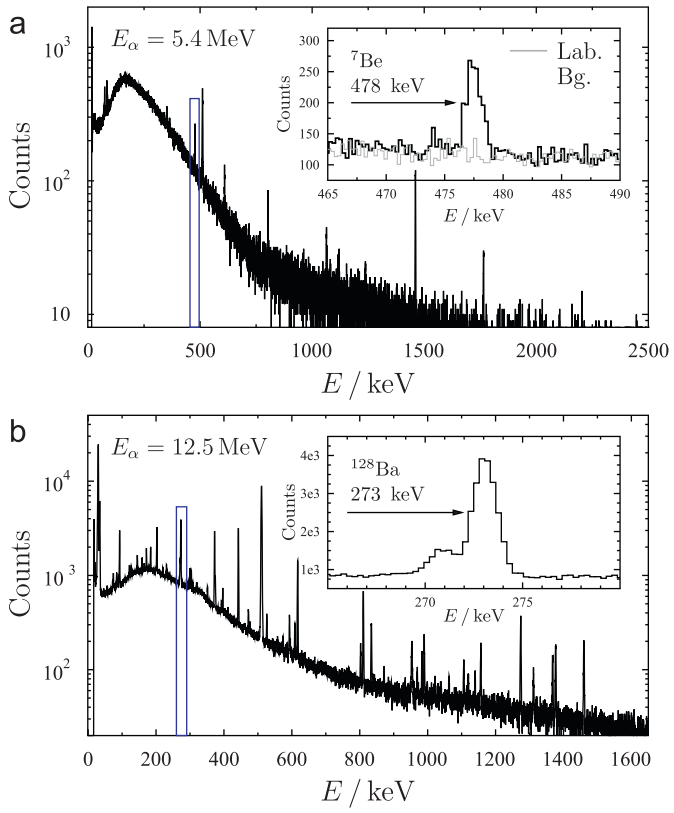

Fig. 6. Activation γ-spectra taken on the catchers used for the two studied reactions. See text for the details. Above: ^{7}Be decay spectrum in the main picture. In the insert part, the 478 keV line along to the laboratory background. Below: the ^{128}Ba spectrum indicating the 273 keV peak in the insert.

peak on ^{124}Xe could well be separated from the lower energy events from inelastic scattering and scattering on the Al foil and beam stop.

4.2. *Detection of the induced* γ-activity

After the irradiations, the catchers were removed from the chamber and transported to the γ-counting setup. This setup consisted of a 100% relative efficiency HPGe detector and a complete 4π low-background shielding. The absolute efficiency of the detector was measured with a set of several calibrated radioactive sources [31]. The calibration sources were approximately point-like, however, the geometry of the ^{7}Be and ^{128}Ba sources were largely different. Due to the angular straggling of the projectiles and the reaction products in the entrance window and the target gas, the produced isotopes were implanted into the catcher in an extended area. GEANT4 [32] simulations were carried out to estimate the distribution of the activity in the catcher. The simulation showed that, for example, in the case of the ^{3}He(α,γ)^{7}Be reaction carried out at 6.5 MeV, 99.7% of the produced ^{7}Be was found within a circular spot of 24 mm in diameter around the beam axis. The obtained distributions were used to simulate the detector efficiency and compared with the point-like source case. Owing to the relatively large solid angle, a typical difference of only 1.0% was found between the point-like and the real case.

Fig. 6 shows the relevant parts of two typical γ-spectra taken on the catchers of the two studied reactions. In the upper panel, the 478 keV peak from the ^{7}Be decay was indicated in the inset. This spectrum was taken for 1 d after irradiating the target by a 5.4 MeV α-beam for 21 h. The laboratory background scaled to the same counting time is also indicated in the inset showing that besides the ^{7}Be peak no increased background was observed. The inset of the lower panel shows the 273 keV peak from the ^{128}Ba decay. In this case the irradiation was done at 12.5 MeV for 15 h and the length of the γ-counting was 1.5 d. In both cases the studied peaks dominated the relevant parts of the spectra showing the feasibility of the activation measurements with the developed gas cells.

5. Summary and conclusion

A thin-window gas cell target was designed and built for the purpose of the cross-section measurements of the astrophysically important reactions ^{3}He(α,γ)^{7}Be and ^{124}Xe(α,γ)^{128}Ba. The gas cell was optimized for activation experiments and to meet the requirements of both reactions. Various measurements were carried out to characterize the most important components of the gas cell system. The first successful test measurement for both reactions showed the feasibility of the cross-section measurements in the desired astrophysically important energy ranges.

Acknowledgments

This work was supported by the European Research Council StG. 203175, HUMAN MB-08-B Mobility Project NKTH-OTKA-EU FP7 (Marie Curie) 82409 and OTKA K101328, and NN83261 (EuroGENESIS).

References

[1] M. Hilgemeier, et al., Zeitschrift für Physik A 329 (1988) 243.
[2] J.L. Osborne, et al., Nuclear Physics A 419 (1984) 115.
[3] T.K. Alexander, et al., Nuclear Physics A 427 (1984) 526.

[4] P.D. Parker, et al., Physical Review 131 (1963) 2578.
[5] K. Nagatani, et al., Nuclear Physics A 128 (1969) 325.
[6] H. Krawinkel, et al., Zeitschrift für Physik A 304 (1982) 307.
[7] R.G.H. Robertson, et al., Physical Review C 27 (1983) 11.
[8] H. Volk, et al., Zeitschrift für Physik A 310 (1983) 91.
[9] D. Bemmerer, et al., Physical Review Letters 97 (2006) 122502.
[10] Gy. Gyürky, et al., Physical Review C 75 (2007) 035805.
[11] F. Confortola, et al., Physical Review C 75 (2007) 065803.
[12] H. Costantini, et al., Nuclear Physics A 814 (2008) 144.
[13] T.A.D. Brown, et al., Physical Review C 76 (2007) 055801.
[14] B.S. Nara Singh, et al., Physical Review Letters 93 (2004) 262503.
[15] A. diLeva, et al., Physical Review Letters 102 (2009) 232502.
[16] M. Arnould, S. Goriely, Physics Report 384 (2003) 1.
[17] T. Rauscher, Physical Review C 73 (2006) 015804.
[18] W. Rapp, et al., Astrophysical Journal 653 (2006) 474.
[19] G.F. Knoll, Radiation Detection and Measurement, Third Edition, John Wiley and Sons, Inc., 2000.
[20] 〈http://www.nndc.bnl.gov/chart/decaysearchdirect.jsp?nuc=7BE&unc=nds〉.
[21] 〈http://www.nndc.bnl.gov/chart/decaysearchdirect.jsp?nuc=128BA&unc=nds〉.
[22] E.K. Warburton, J.W. Olness, C.J. Lister, Physical Review C 20 (1979) 619.
[23] S. Saude, et al., Nuclear Instruments and Methods in Physics Research Section B 216 (2004) 156.
[24] J.E. Doskow, F. Sperisen, Nuclear Instruments and Methods in Physics Research Section A 362 (1995) 20.
[25] T. Botto, et al., Nuclear Instruments and Methods in Physics Research Section A 362 (1995) 26.
[26] 〈http://www.lebowcompany.com/〉.
[27] 〈http://www.goodfellow.com〉.
[28] 〈http://www.ortec-online.com/〉.
[29] J.F. Ziegler, J.P. Biersack, SRIM Code 〈http://www.srim.org〉.
[30] 〈http://www.advent-rm.co 〉.
[31] Z. Halász, et al., Physical Review C 85 (2012) 025804.
[32] S. Agostinelli, et al., Nuclear Instruments and Methods in Physics Research Section A 506 (2003) 250.